Chemical and Process Engineering Research
ISSN 2224-7467 (Paper) ISSN 2225-0913 (Online)
Vol.49, 2017

Chemically Reacting Radiative Casson Fluid Flow over a Vertical Plate in the Presence of a Heat Source/Sink and Aligned Magnetic Field

R. Vijayaragavan* M. Angeline Kavitha
Department of Mathematics, Thiruvalluvar University, Vellore-632 115, India

Abstract
In this study, we investigated the heat and mass transfer characteristics of the MHD Casson fluid flow over a vertical plate in the presence of thermal radiation, chemical reaction and heat source/sink with buoyancy effects. The aligned magnetic field is applied along the flow direction. The governing partial differential equations are transformed as non-dimensional ODE's using suitable transformation and resulting equations are solved using Perturbation technique. The effects of various non-dimensional governing parameters, namely thermal radiation, chemical reaction, heat source/sink, Prandtl number, Grashof number, magnetic field parameter, inclined angle parameter and slip parameter on the flow, mass and heat transfer is analyzed for both Casson and Newtonian fluid cases. Also the friction factor, the local Nusselt number and Sherwood number are discussed and presented graphically. It is found that aligned magnetic field parameter has tendency to control the flow and thermal field.
Keywords: MHD, Casson fluid, thermal radiation, heat source/sink, buoyancy effect, chemical reaction.

1. Introduction

Fluid dynamics mainly deal with the study of flow behavior in different channels. The effect of radiation on MHD flows have numerous applications in power generators and also it plays a special role in the field of geophysics and astrophysics. Reddy et al. [1] investigated the Casson fluid flow past an upper surface of a paraboloid of revolution in the presence of magnetic nonoparticles. Through this paper, they discern that Nusselt number increases effectively through higher values of Biot number. Sandeep et al. [2], analyzed 3D-Casson fluid flow over a stagnation point in the presence of cross diffusion. In this study, they used Runge-Kutta method with shooting technique. The effect of 3D MHD Casson fluid flow past a stretching sheet in the presence of thermophoresis and Brownian motion was deliberated by Sulochana et al. [3]. The researchers [4-9] investigated the heat and mass transfer nature of the Newtonian and non-Newtonian fluids by considering various flow geometries.

Ali and Sandeep [10], analyzed the effects of radiative heat transfer in MHD Casson-ferrofluid through different geometries and found that the heat transfer rate is greater in the flow over a cone when compared with the flow over a plate and a wedge. The heat and mass transfer behavior of MHD Newtonian and non-Newtonian flows past a cone or plate with Diffusion was deliberated by the researchers [11, 12]. The flow and heat transfer behavior of liquid film flow of non-Newtonian nanofluids in the presence of grapheme nanoparticles was investigated by Sandeep and Malvandi [13]. Hayat et al. [14] analyzed the flow of Casson fluid with nanoarticles. In this article they found that when the strength of the Brownian motion enhances the temperature decreases. Hayat et al. [15] elaborated the concept of mixed convective stagnation point flow of Casson fluid under the effect of convective boundary conditions. The Heat and Mass transfer behavior of non-Newtonian fluid through stretching sheet was studied by Nadeem et al. [16]. Pramanik [17] analyzed the concept of Casson fluid flow and heat transfer over a porous exponentially stretching sheet in the presence of thermal radiation. Sarojamma et al. [18] discussed the heat and mass transfer behavior of a MHD Casson fluid over a parallel plate with stretching walls. In this paper they used Runge-Kutta fourth order shooting method. Arthur et al. [19] investigated Casson fluid flow past a vertical porous surface in the presence of a magnetic field.

The heat transfer of nonlinear radiative magnetohydrodynamic Cu-water nanofluid flow over two different geometries was studied by Sandeep et al.[20]. Harinath Reddy et al. [21] elaborated the study of MHD Casson fluid flow over an oscillating vertical plate in the presence of radiation absorption. In this study, they found that when chemical reaction parameter enhances the concentration of the Casson fluid decreases. Haritha and Sarojamma [22] analyzed the influence of thermal radiation on heat and mass transfer in MHD Casson fluid flow past a stretching sheet. Sathies Kumar and Gangadhar [23] discussed the effects of viscous dissipation and partial slip on three dimensional MHD flow of Casson fluid through a permeable sheet. In this study they used shooting technique and concluded that when convective parameter increases thermal boundary layer thickness increases significantly.Sharada and Shankar [24] elaborated the study deals with the MHD mixed convection flow of a Casson fluid past an exponentially stretching sheet with Soret and Dufour. In this study, they resulted that the temperature enhances with enhancing values of the Dufour number and radiation parameter. Peristaltic transport of a Casson fluid in an inclined channel was investigated by Nagarani [25]. Ganesh et al. [26] discussed the two-dimensional flow of a Casson fluid between parallel plates. Mixed convection stagnation point flow of

an incompressible Casson fluid past a stretching sheet with the convective boundary condition was analyzed by Mahanta and Shaw [27]. Two-dimensional flow of a Casson fluid past a stretching sheet was studied by Kirubhashankar et al. [28] . Mahdy and Chamkha [29] discussed the unsteady two-dimensional flow of a non-Newtonian nanofluid through a contracting cylinder using Buongiorno's model. Vedavathi et al. [30] investigated the Dufour and radiation effects in MHD Casson fluid flow past a vertical plate with heat source/sink. In this article they used perturbation technique and discussed the effects of different physical parameters. Afikuzzaman et al. [31] exhibited the study of Casson fluid flow over a parallel plate with Hall Current. The steady Squeezing flow of Casson fluid between parallel plates was analyzed by Ahmed et al. [32]. Very recently, the researchers [33-36] analyzed the heat and mass transfer behavior of magnetohydrodynamic flows.

With the help of the above studies, in this study, we investigated the heat and mass transfer characteristics of the MHD Casson fluid flow over a vertical plate in the presence of thermal radiation, chemical reaction and heat source/sink with buoyancy effects. The aligned magnetic field is applied along the flow direction. The governing partial differential equations are transformed as non-dimensional ODE's using suitable transformation and resulting equations are solved using Perturbation technique. The effects of various non-dimensional governing parameters, namely thermal radiation, chemical reaction, heat source/sink, Prandtl number, Grashof number, magnetic field parameter, inclined angle parameter and slip parameter on the flow, mass and heat transfer is analyzed for both Casson and Newtonian fluid cases.

2. Formulation of the problem

Consider a 2D unsteady flow of Casson fluid over a semi-infinite vertical plate. Here the plate is placed along $\bar{x}$ -axis and $\bar{y}$ axis is normal to it. An inclined magnetic field of strength B_0 is considered as depicted in Fig.1. Internal heat source/sink, thermal radiation and chemical reaction effects are taken into account. Suction velocity is considered as $\bar{v} = -V_0\left(1+\varepsilon A e^{\bar{n}\bar{t}}\right)$, where A >0, ε and εA are small quantities less than unity and $V_0 > 0$. We ignored the induced magnetic field and viscous dissipation effects. With the assumptions made above, the governing conservative equations are as follows:

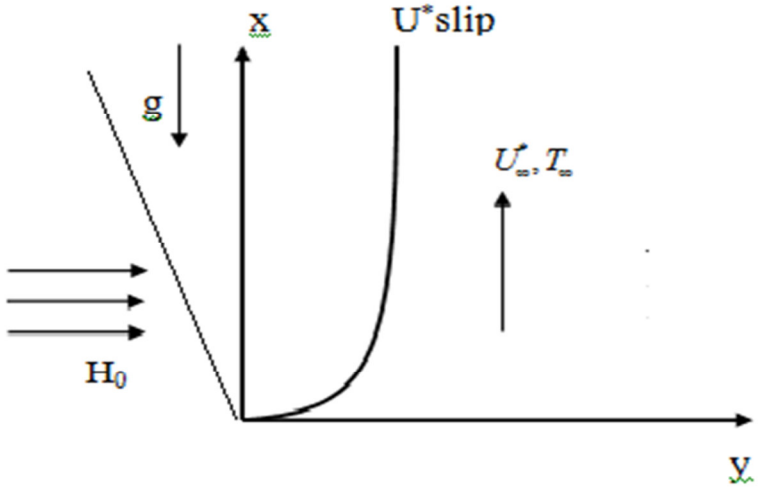

Fig.1 Physical model and the coordinate system.

Continuity:

$$\frac{\partial \bar{v}}{\partial \bar{y}} = 0, \tag{1}$$

Momentum:

$$\frac{\partial \bar{u}}{\partial \bar{t}} + \bar{v}\frac{\partial \bar{u}}{\partial \bar{y}} = -\frac{1}{\rho}\frac{\partial \bar{p}}{\partial \bar{x}} + \nu\left(1+\frac{1}{\beta}\right)\frac{\partial^2 \bar{u}}{\partial \bar{y}^2} + g\beta_T\left(\bar{T}-T_\infty\right) + g\beta_C\left(\bar{C}-C_\infty\right) - \frac{\sigma B_0^2}{\rho}\bar{u}\sin^2\gamma, \tag{2}$$

Energy:

$$\frac{\partial \bar{T}}{\partial \bar{t}}+\bar{v}\frac{\partial \bar{T}}{\partial \bar{y}}=\frac{k}{\rho c_p}\frac{\partial^2 \bar{T}}{\partial \bar{y}^2}-\frac{1}{\rho cp}\frac{\partial \bar{q}_r}{\partial \bar{y}}-\frac{Q_0}{\rho c_p}\left(\bar{T}-T_\infty\right), \tag{3}$$

Concentration:

$$\frac{\partial \bar{C}}{\partial \bar{t}}+\bar{v}\frac{\partial \bar{C}}{\partial \bar{y}}=D\frac{\partial^2 \bar{C}}{\partial \bar{y}^2}-k_l\left(\bar{C}-C_\infty\right), \tag{4}$$

where the velocity components along $\bar{x}$ and $\bar{y}$ directions are $\bar{u}$ and $\bar{v}$. The radiative heat flux is defined as follows

$$\frac{\partial \bar{q}_r}{\partial \bar{y}}=4\left(\bar{T}-T_\infty\right)\bar{I}, \tag{5}$$

where $\bar{I}=\int K_{\lambda w}\frac{\partial e_{b\lambda}}{\partial \bar{T}}d\lambda$

The boundary conditions are as follows

$$\left.\begin{aligned}&\bar{u}=\bar{u}_{slip}=\phi_1\frac{\partial \bar{u}}{\partial \bar{y}},\bar{T}=T_w,\bar{C}=C_w \quad at\ \ \bar{y}=0,\\&\bar{u}\to\bar{u}_\infty=U_0\left(1+\varepsilon e^{\bar{n}\bar{t}}\right),\bar{T}\to T_\infty,\bar{C}\to C_\infty \ \ as\ \ \bar{y}\to\infty,\end{aligned}\right\} \tag{6}$$

In Eq. (2) applied pressure gives

$$-\frac{1}{\rho}\frac{d\bar{p}}{d\bar{x}}=\frac{d\bar{U}_\infty}{d\bar{t}}+\frac{\sigma B_0^2}{\rho}\bar{U}_\infty\sin^2\alpha, \tag{7}$$

Now, we introduce the dimensionless variables as follows

$$u=\frac{\bar{u}}{U_0},v=\frac{\bar{v}}{V_0},y=\frac{V_0\bar{y}}{v},U_\infty=\frac{\bar{U}_\infty}{U_0},t=\frac{\bar{t}V_0^2}{v},\theta=\frac{\bar{T}-T_\infty}{T_w-T_\infty},\phi=\frac{\bar{C}-C_\infty}{C_w-C_\infty},$$

$$n=\frac{\bar{n}v}{V_0^2},\Pr=\frac{\mu c_p}{k},M=\frac{\sigma B_0^2}{\rho V_0^2},Gr=\frac{v\beta g(T_w-T_\infty)}{U_0V_0^2},Gc=\frac{v\beta g(C_w-C_\infty)}{U_0V_0^2}, \tag{8}$$

$$F=\frac{4v\bar{I}}{\rho c_pV_0^2},Sc=\frac{v}{D},Kr=\frac{vk_l}{V_0^2},\mathrm{S}=\frac{Q_0v}{\rho c_pV_0^2},\phi_1=\frac{\sqrt{k}}{\alpha}U_0$$

Using (8), the governing Eqs. (2) to (4) reduce as:

$$\frac{\partial u}{\partial t}-\left(1+Ae^{nt}\right)\frac{\partial u}{\partial y}=\frac{dU_\infty}{dt}+\left(1+\frac{1}{\beta}\right)\frac{\partial^2 u}{\partial y^2}+Gr\theta+Gc\phi+M\left(U_\infty-u\right)\sin^2\gamma, \tag{9}$$

$$\frac{\partial \theta}{\partial t}-\left(1+Ae^{nt}\right)\frac{\partial \theta}{\partial y}=\frac{1}{\Pr}\frac{\partial^2\theta}{\partial y^2}-F\theta-S\theta \tag{10}$$

$$\frac{\partial C}{\partial t}-\left(1+Ae^{nt}\right)\frac{\partial \phi}{\partial y}=\frac{1}{Sc}\frac{\partial^2\phi}{\partial y^2}-Kr\phi, \tag{11}$$

The transformed boundary conditions are

$$\left.\begin{aligned}&u=u_{slip}=\phi_1\frac{\partial u}{\partial y},\theta=1,\phi=1, \quad at\ \ y=0,\\&u\to U_\infty=1+\varepsilon e^{nt},\theta\to 0,\phi\to 0 \quad as\ \ y\to\infty,\end{aligned}\right\} \tag{12}$$

Solution of the problem

To solve the equations (9) to (11), we assume the solution in the following form:

$$u=f_0\left(y\right)+\varepsilon e^{nt}f_1\left(y\right)+O\left(\varepsilon^2\right), \tag{13}$$

$$\theta = g_0(y) + \varepsilon e^{nt} g_1(y) + O(\varepsilon^2), \tag{14}$$

$$\phi = h_0(y) + \varepsilon e^{nt} h_1(y) + O(\varepsilon^2), \tag{15}$$

Substituting Eqs. (13) to (15) into the equations (9) to (11) and equating the harmonic and non-harmonic terms, neglecting the coefficient of $O(\varepsilon^2)$, we have

$$Bf_o'' + f_0' - M\sin^2\gamma f_0 = -M\sin^2\gamma - Grg_0 - Gch_0, \tag{16}$$

$$Bf_1'' + f_1' - (M\sin^2\gamma + n)f_1 = -Af_0' - Grg_1 - Gch_1 - (M\sin^2\gamma + n), \tag{17}$$

$$g_0'' + \Pr g_0' - \Pr(F+S)g_0 = 0 \tag{18}$$

$$g_1'' + \Pr g_1' - \Pr(F+S+n)g_1 = -A\Pr g_0' \tag{19}$$

$$h_0'' + Sch_0' - KrSch_0 = 0, \tag{20}$$

$$h_1'' + Sch_1' - Sc(Kr+n)h_1 = -Sch_0', \tag{21}$$

The corresponding boundary conditions are

$$\left.\begin{aligned} f_0 = \frac{\sqrt{k}}{\alpha}U_0 f_0', f_1 = \frac{\sqrt{k}}{\alpha}U_0 f_1', g_0 = 1, g_1 = 0, h_0 = 1, h_1 = 0 \quad at\ y = 0, \\ f_0 = 0, f_1 = 1, g_0 \to 1, g_1 \to 0, h_0 \to 1, h_1 \to 0 \qquad as\ \ y \to \infty, \end{aligned}\right\} \tag{22}$$

The solution of equations (16)-(21) with the boundary conditions Eq. (22) are

$$f_0(y) = 1 + D_3 e^{-m_3 y} + D_2 e^{-m_1 y}, \tag{23}$$

$$f_1(y) = 1 + D_7 e^{-m_4 y} + D_4 e^{-m_3 y} + D_5 e^{-m_2 y} + D_6 e^{-m_1 y}, \tag{24}$$

$$g_0(y) = e^{-m_1 y} \tag{25}$$

$$g_1(y) = D_1 e^{-m_2 y} + D_1 e^{-m_1 y} \tag{26}$$

$$h_0(y) = e^{-m_5 y} \tag{27}$$

$$h_1(y) = D_8 e^{-m_6 y} + D_8 e^{-m_5 y} \tag{28}$$

Substituting the equations (23) - (28), in Eqs. (13) to (15), we obtain the velocity, temperature and concentration distributions as follows:

$$u(y,t) = 1 + D_3 e^{-m_3 y} + D_2 e^{-m_1} + \varepsilon e^{nt}\begin{pmatrix} 1 + D_7 e^{-m_4 y} + D_4 e^{-m_3 y} \\ + D_5 e^{-m_2 y} + D_6 e^{-m_1 y} \end{pmatrix}, \tag{29}$$

$$\theta(y,t) = e^{-m_1 y} + \varepsilon e^{nt}\left(-D_1 e^{-m_2 y} + D_1 e^{-m_1 y}\right), \tag{30}$$

$$\phi(y,t) = e^{-m_5 y} + \varepsilon e^{nt}\left(-D_8 e^{-m_6 y} + D_8 e^{-m_5 y}\right), \tag{31}$$

Where

$$m_1=\frac{\Pr+\sqrt{\Pr^2+4\Pr(F+S)}}{2},\ m_2=\frac{\Pr+\sqrt{\Pr^2+4\Pr(F+S+n)}}{2},$$

$$m_3=\frac{1}{2}\left(1+\sqrt{1+4BM\sin^2\gamma}\right),m_4=\frac{1}{2}\left(1+\sqrt{1+4B(n+M\sin^2\gamma)}\right),$$

$$m_5=\frac{Sc+\sqrt{Sc^2+4ScKr}}{2},m_6=\frac{Sc+\sqrt{Sc^2+4Sc(Kr+n)}}{2},$$

$$D_1=\frac{A\Pr m_1}{m_1^2-\Pr m_1-(F+S+n)\Pr},D_2=\frac{-Gr}{Bm_1^2-m_1-M\sin^2\gamma},$$

$$D_3=\frac{-(1+D_2+\phi_1 m_1 D_2)}{1+\phi_1 m_3},\ D_4=\frac{AD_3m_3}{Bm_3^2-m_3-(M\sin^2\gamma+n)},\phi_1=\frac{\sqrt{k}}{\alpha}U_0,$$

$$D_5=\frac{GrD_1}{Bm_2^2-m_2-(M\sin^2\gamma+n)},D_6=\frac{AD_2m_1-GrD_1}{Bm_1^2-m_1-(M\sin^2\gamma+n)},$$

$$D_7=\frac{-(1+D_4+D_5+D_6)-\phi_1(D_4m_3+D_5m_2+D_6m_1)}{1+\phi_1m_4},$$

$$D_8=\frac{A\Pr m_5}{m_5^2-Scm_5-(Kr+n)Sc},$$

Skin friction at the wall is given by

$$C_{fx}=\frac{\tau_w}{\rho U_0V_0}=\left.\frac{\partial u}{\partial y}\right|_{y=0}$$

$$C_{fx}=-(D_3m_3+D_2m_1)-\varepsilon e^{nt}(D_7m_4+D_4m_3+D_5m_2+D_6m_1)$$

Nusselt number is given by

$$Nu_x=x\frac{\left.\frac{\partial T}{\partial y}\right|_w}{T_w-T_\infty}\Rightarrow Nu_x/\mathrm{Re}_x=\left.\frac{\partial\theta}{\partial y}\right|_{y=0}$$

$$Nu_x/\mathrm{Re}_x=-m_1+\varepsilon e^{nt}D_1(m_2-m_1)$$

Sherwood number is given by

$$Sh_x=x\frac{\left.\frac{\partial C}{\partial y}\right|_w}{T_w-T_\infty}\Rightarrow Sh_x/\mathrm{Re}_x=\left.\frac{\partial\phi}{\partial y}\right|_{y=0}$$

$$Sh_x/\mathrm{Re}_x=-m_5+\varepsilon e^{nt}D_8(m_6-m_5)$$

Where $\mathrm{Re}_x=\frac{V_0x}{\nu}$ is the Reynolds number.

3. Results and Discussion

The obtained results show the effects of the various non-dimensional governing parameters namely, Chemical reaction, Thermal radiation, Heat source/sink, Prandtl number, Grashof number, Schmidt number, Porosity parameter, inclined angle parameter and Magnetic field parameter on the flow and heat transfer for both Newtonian and Casson fluid cases. Also discussed the local Nusselt number, friction factor and Sherwood number for both cases. For graphical results we used the non-dimensional parameter values as Gr=5, Pr=6, Kr=0.2, Sc=0.6, M=3,K=1,S=0.5, F=1, n=1, t=1, Ɛ=0.2, ϕ_1 =0.3**.** These values are kept as common in the entire study except the Variations displayed in respective figures.

Fig.2 exhibits the effects of Magnetic field parameter M on velocity profiles. It is noticed that increasing the Magnetic field parameter enhances the velocity profiles of both fluids. The effect of Prandtl number Pr on velocity profiles is displayed in Fig.3. It is evident that increasing values of Prandtl number

decrease the velocity profiles of both non-Newtonian and Newtonian fluids.

Fig.4 which shows that the rising value of time t implies the increase in velocity profiles of both fluids. The effect of Grashof number Gr on velocity profiles is displayed in Fig.5. The result shows that increasing values of Grashof number enhances the velocity profiles of both fluids. Fig.6 represents the effect of radiation parameter F on velocity profile. It is observed that rising values of radiation parameter F lead to a decrease in the velocity profiles of both fluids.Fig.7 shows that the effect of slip ϕ_1 parameter on velocity profiles. The result shows that the rising value of slip parameter increases the non-Newtonian fluid and decreases the Newtonian fluid.

Fig.8 depicts the effect of heat source parameter S on velocity profile. We noticed that an increasing value of heat source parameter S decreases the velocity profile for both Newtonian and non-Newtonian fluids. The velocity profile for several values of are shown in Fig.9. It is observed that an increase in the value enhances the velocity profiles of both Newtonian fluid and non-Newtonian fluid near the boundary. The effect of inclined angle parameter γ on velocity profile is displayed in Fig.10. It is evident that increasing values of inclined angle parameter γ lead to a decrease in the momentum boundary layer.

Fig.11 illustrate the temperature profile for different values of ε. It is noticed that the rising value of ε decreases the temperature boundary layer. Fig.[12-14] are plotted to depict the variation of temperature profiles for different values of radiation parameter F, Prandtl number Pr and heat source parameter S. This shows that, an increase in the radiation parameter F, Prandtl number Pr and heat source parameter S imply the decrease in temperature profile.

Fig.15 represents the effect of heat source parameter S against the magnetic field parameter M on the skin friction coefficient. The result shows that rising the heat source parameter against the magnetic field parameter enhance the skin friction coefficient. Fig.16 and Fig.18 shows the variation in friction factor with the increase in heat source parameter S and slip parameter ϕ_1 against the radiation parameter F. It is observed that rising values of heat source parameter S and slip parameter ϕ_1 with increasing values of F tend to gradual decrease in the skin friction coefficient.

Fig.17 shows the effect of Prandtl number Pr against the heat source parameter F on the skin friction coefficient. The result shows that increasing the Prandtl number against the heat source parameter F decreases the skin friction coefficient. Fig.19 and Fig.20 depicts the effect of Prandtl number Pr against the radiation parameter F and heat source parameter S on Nusselt number. It is observed that increasing the Prandtl number Pr against the radiation parameter F and heat source parameter S decreases the Nusselt number. Fig.21 illustrates the effect of radiation parameter F against the heat source parameter S on Nusselt number. This figure results that rising values of radiation parameter F against the heat source parameter S reduces the Nusselt number.

The effects of Chemical reaction parameter Kr and Schmidt number Sc on concentration profiles are shown in Fig.22 and Fig.23. It is noticed that increasing values of Chemical reaction parameter Kr and Schmidt number Sc leads to a gradual decrease in the concentration profiles. Fig.24 represents the effect of Chemical reaction parameter Kr against the Schmidt number Sc on Sherwood number. It is observed that the rising values of Chemical reaction parameter Kr against the Schmidt number implies the decrease in Sherwood number.

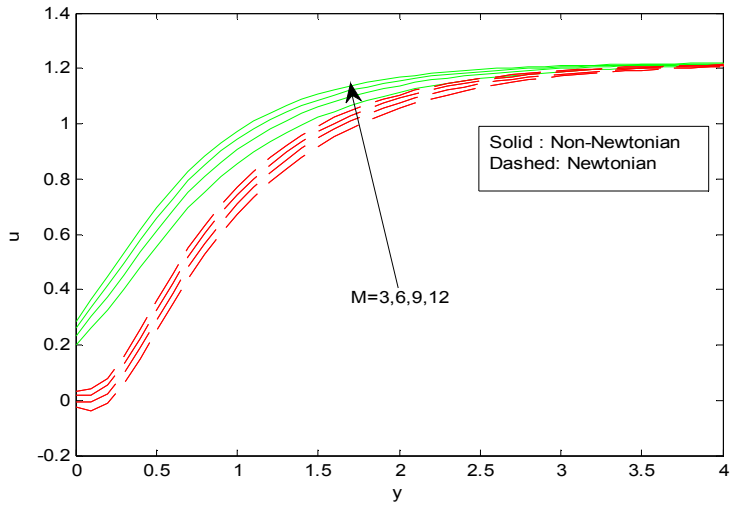

Fig .2 Velocity profiles for different values of Magnetic field parameter.

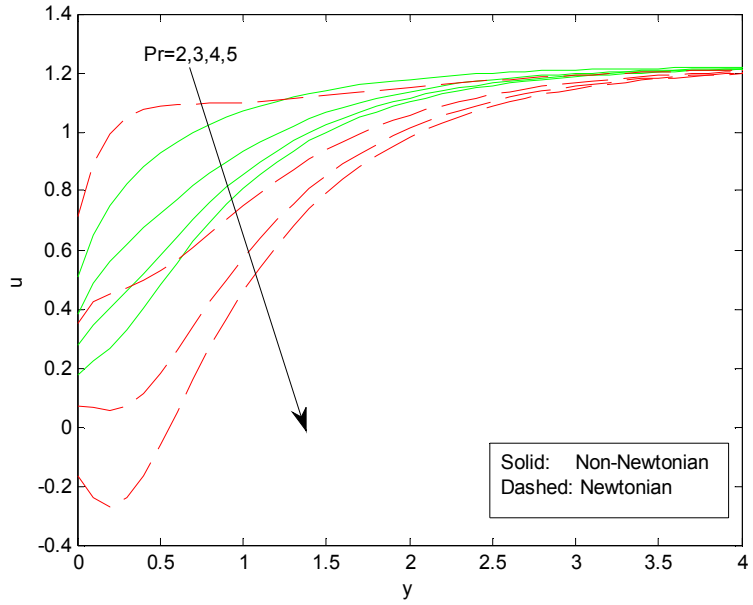

Fig .3 Velocity profiles for different values of Prandtl number.

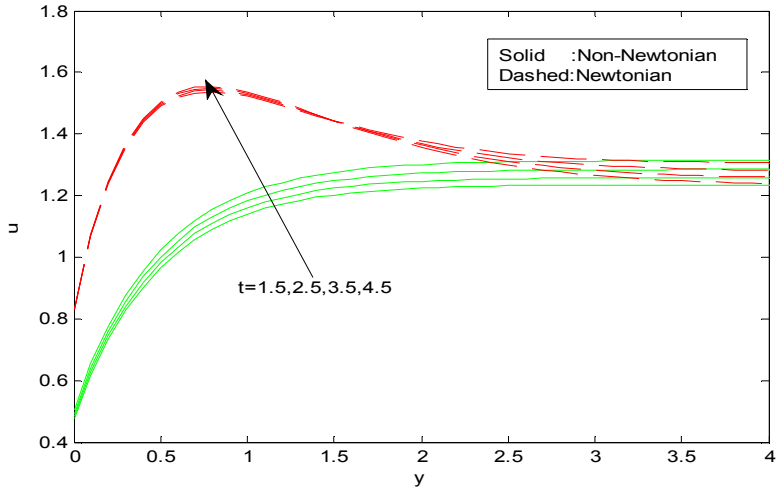

Fig .4 Velocity profiles for different values of time.

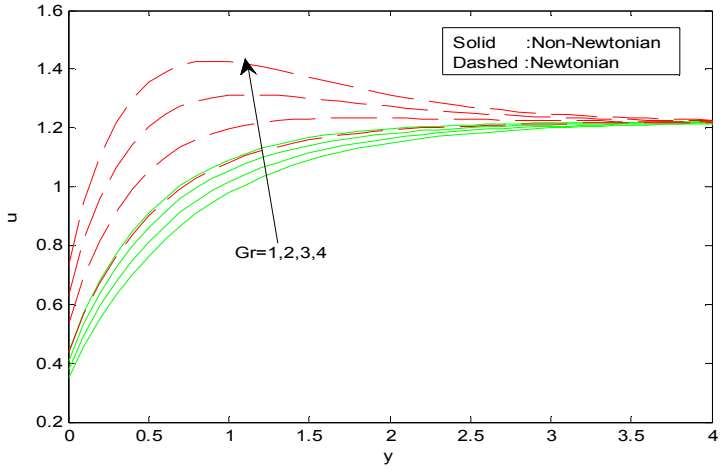

Fig .5 Velocity profiles for different values of Grashof number .

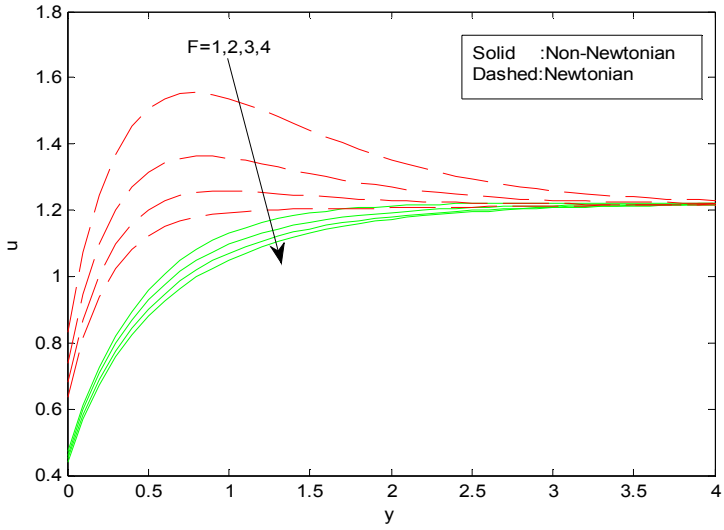

Fig .6 Velocity profiles for different values of radiation parameter.

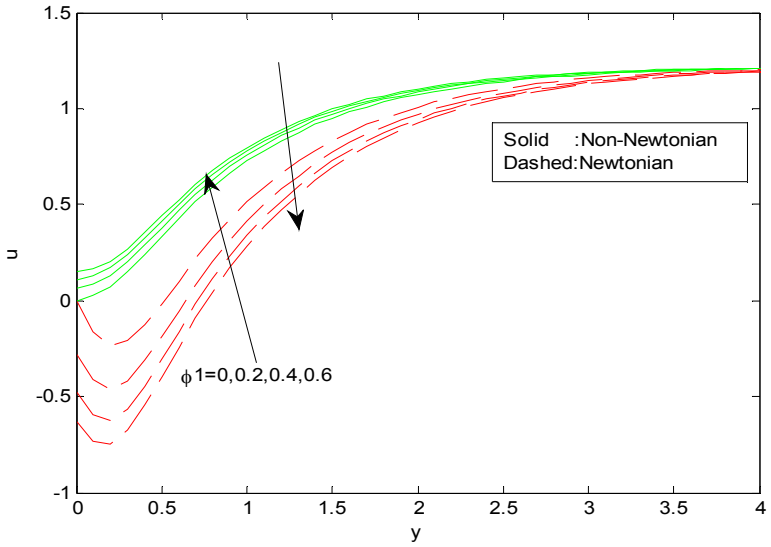

Fig .7 Velocity profiles for different values of Slip parameter.

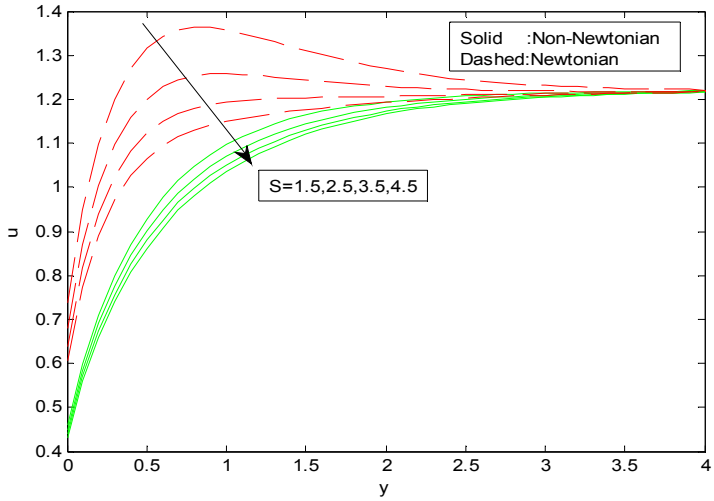

Fig .8 Velocity profiles for different values of Heat Source parameter.

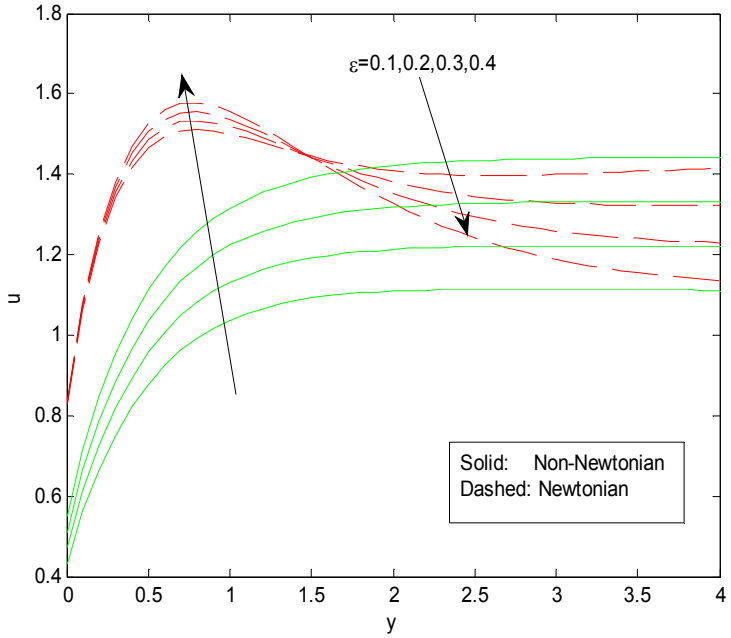

Fig .9 Velocity profiles for different values of

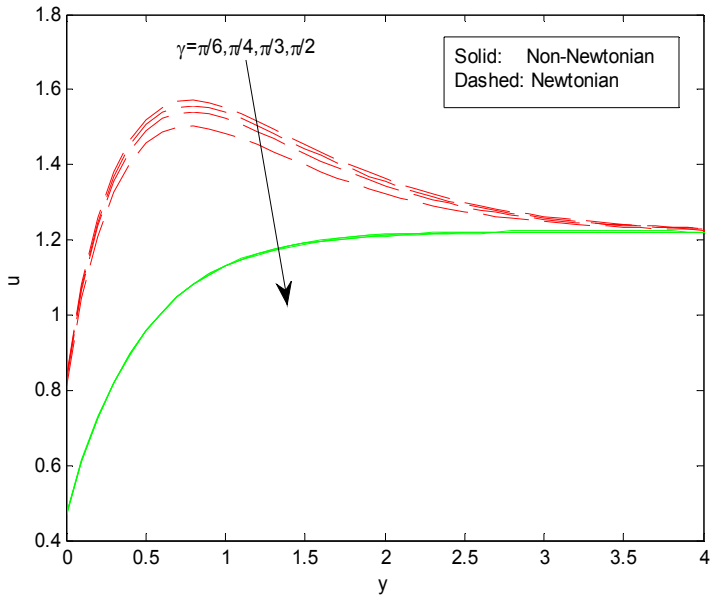

Fig .10 Velocity profiles for different values of inclined angle parameter.

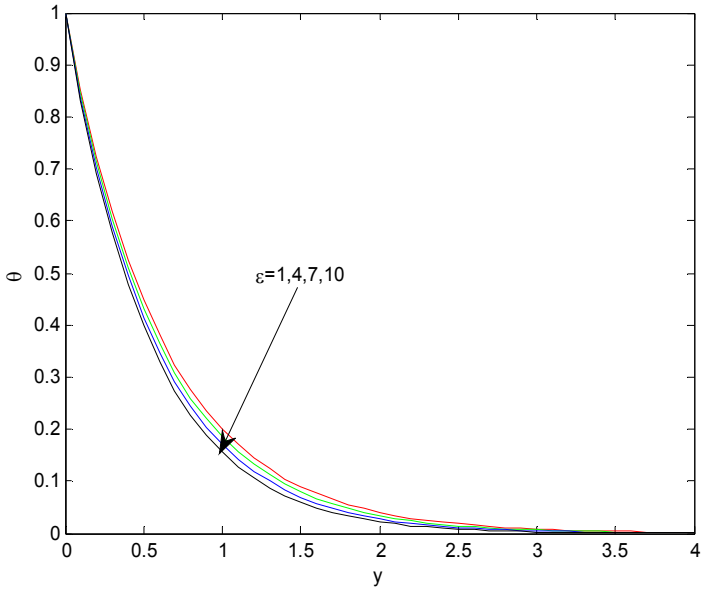

Fig .11 Temperature profiles for different values of .

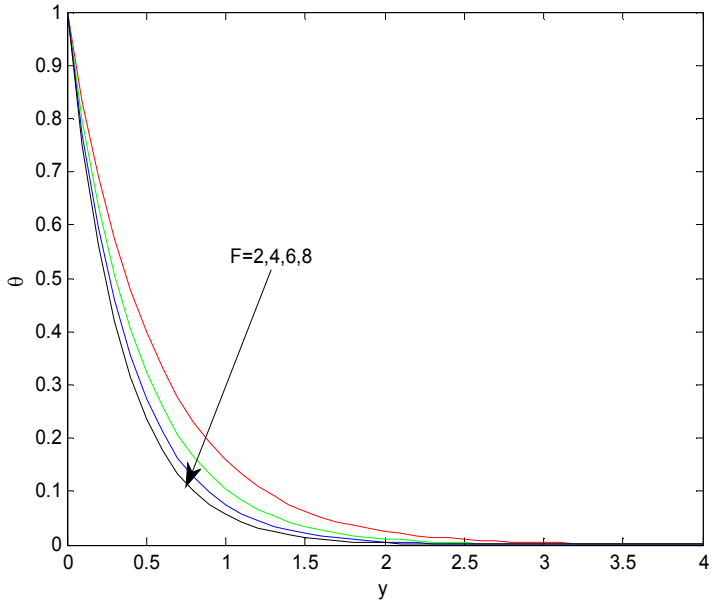

Fig .12 Temperature profiles for different values of radiation parameter.

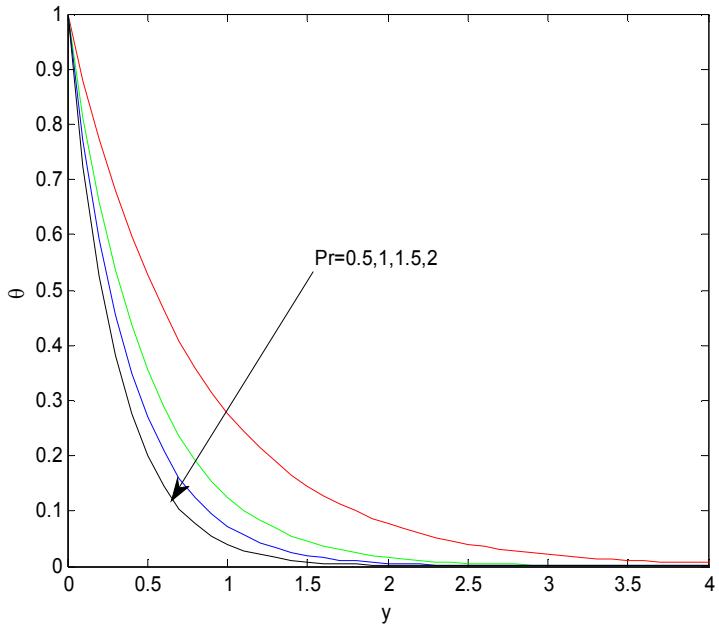

Fig .13 Temperature profiles for different values of Prandtl number.

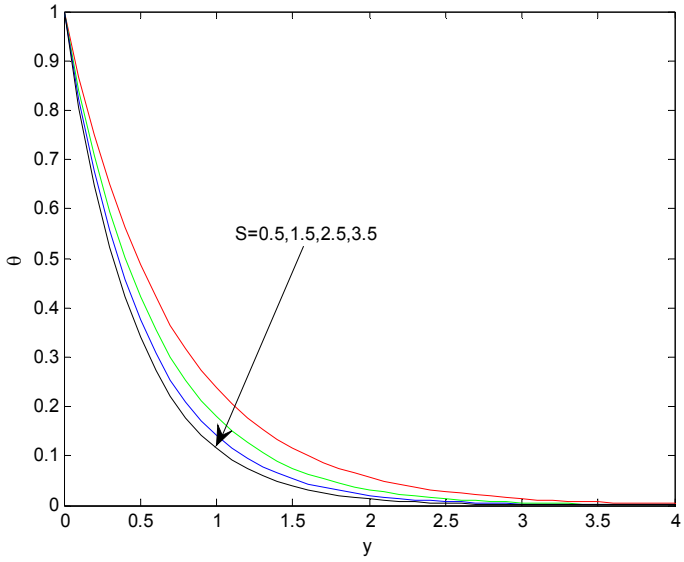

Fig .14 Temperature profiles for different values of Heat Source parameter.

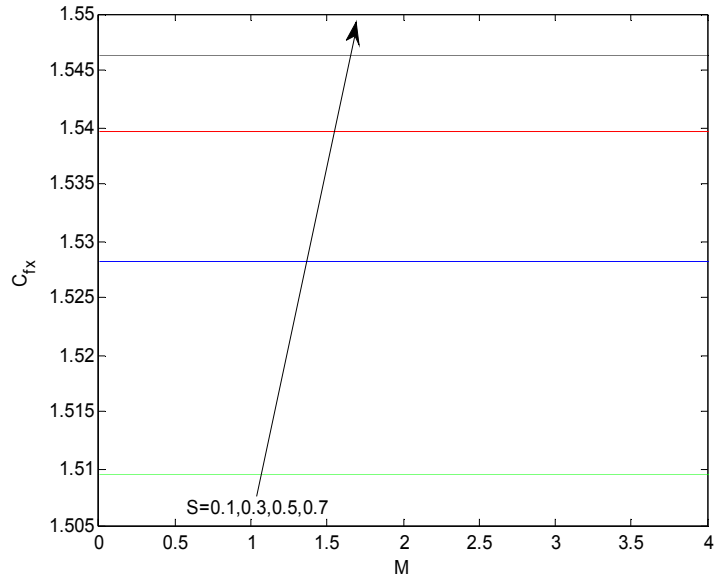

Fig .15 Variations in skin friction coefficient for different values of S with M.

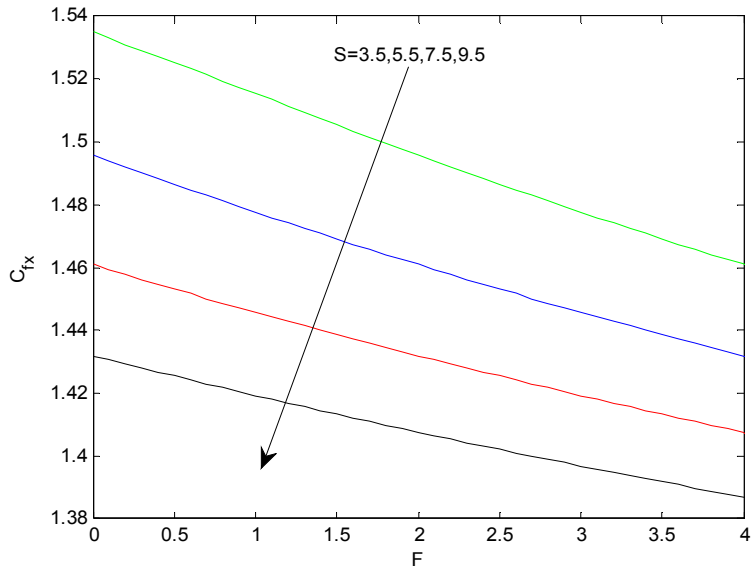

Fig .16 Variations in skin friction coefficient for different values of S with F.

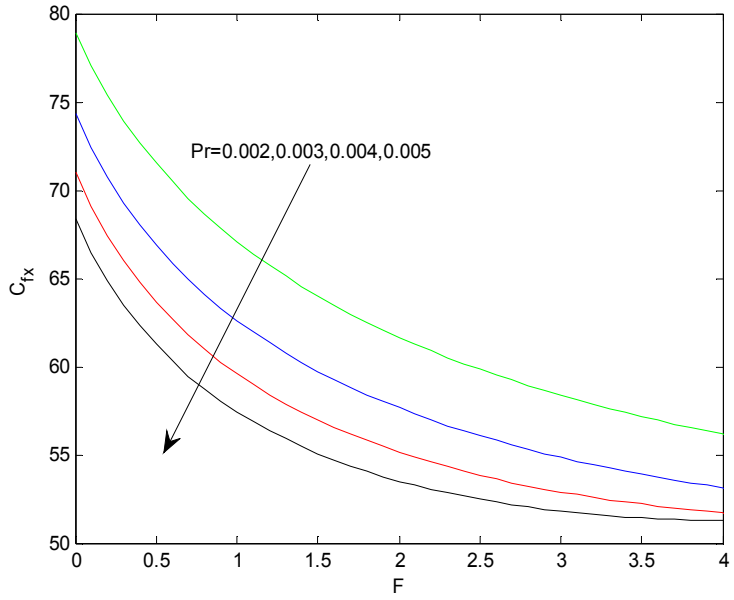

Fig .17 Variations in skin friction coefficient for different values of Pr with F.

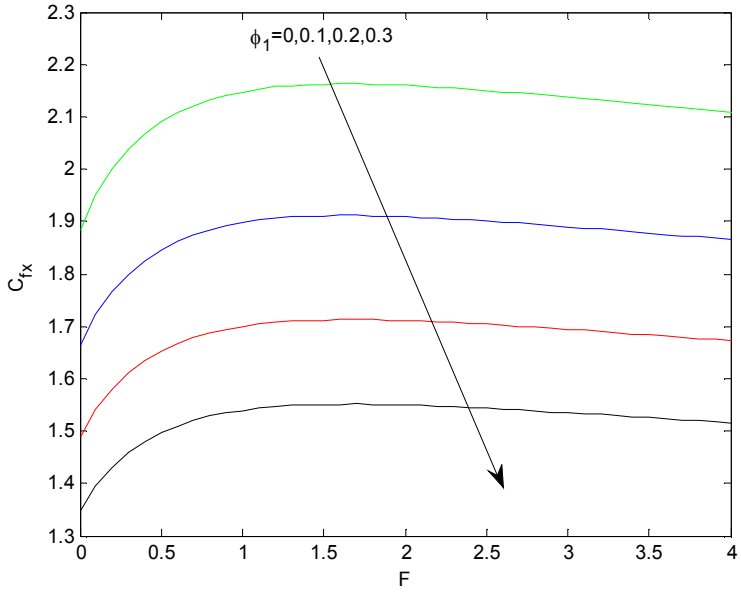

Fig .18 Variations in skin friction coefficient for different values of ϕ_1 with F.

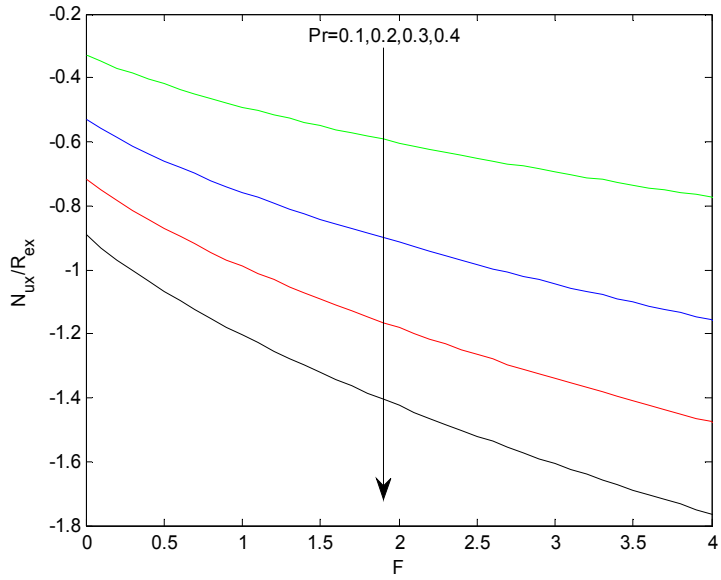

Fig .19 Variations in Nusselt number for different values of Pr with F.

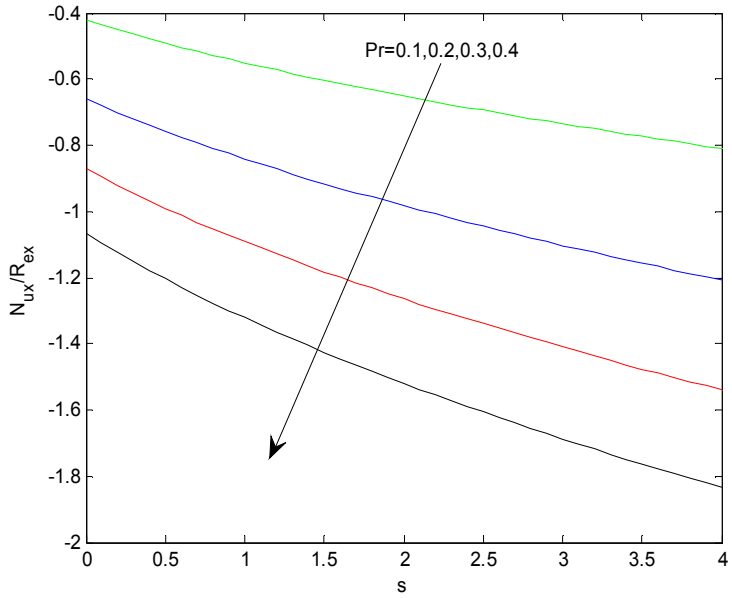

Fig .20 Variations in Nusselt number for different values of Pr with S.

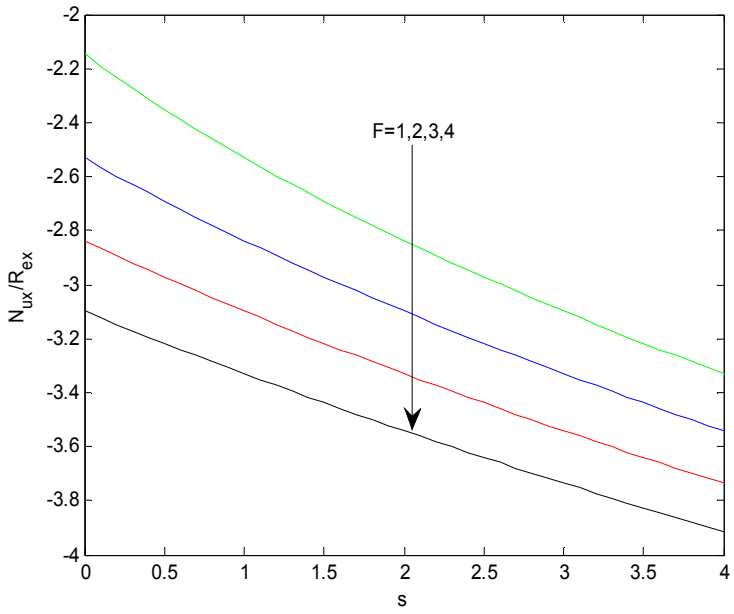

Fig .21 Variation in Nusselt number for different values of F with S.

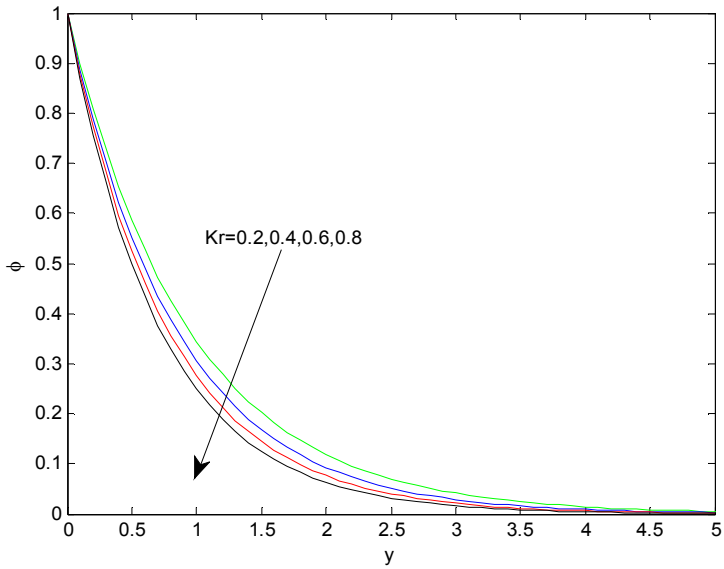

Fig .22 Concentration profiles for different values of Chemical reaction parameter.

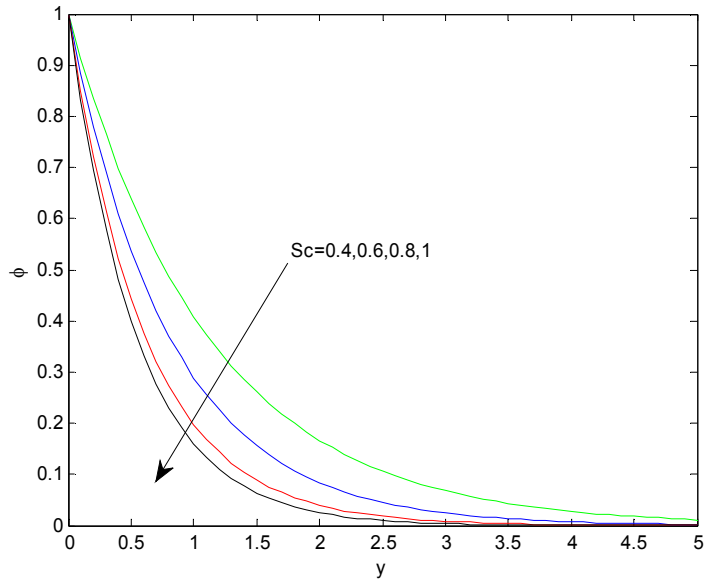

Fig .23 Concentration profiles for different values of Schmidt number.

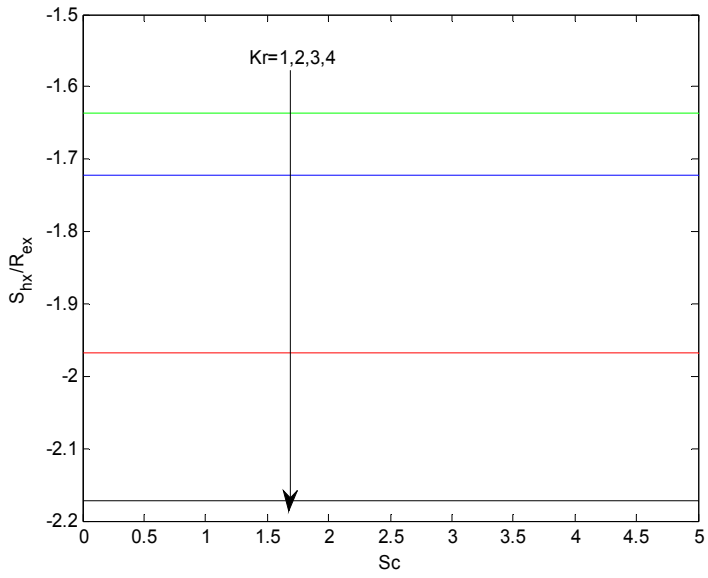

Fig .24 Variations in Sherwood number for different values of Kr with Sc.

4. Conclusions

Heat and mass transfer characteristics of the MHD Casson fluid flow over a vertical plate in the presence of thermal radiation, chemical reaction and heat source/sink with buoyancy effects are analyzed theoretically. The aligned magnetic field is applied along the flow direction. The governing partial differential equations are transformed as non-dimensional ODE's using suitable transformation and resulting equations are solved using Perturbation technique. The effects of various non-dimensional governing parameters on flow, thermal and concentration fields are discussed and analyzed. The observations of the present study are as follows:

- Aligned angle controls the applied magnetic field strength and hence the flow field.
- Buoyancy effects enhance the heat transfer rate.
- Slip effect declines the velocity field of Casson fluid and enhances the flow field of regular fluid.
- Rising values of heat source/sink parameter depreciate the temperature filed and enhances the heat transfer rate.
- Increasing values of chemical reaction and Schmidt number declines the concentration filed and enhances the mass transfer rate.

References

[1]. J.V. Ramana Reddy, V. Sugunamma and N.Sandeep. Enhanced heat transfer in the flow of dissipative non-Newtonian Casson fluid flow over a convectively heated upper surface of a paraboloid of revolution. Journal of Molecular liquids 229 (2017) 380-388.
[2]. Naramgari Sandeep, Olubode Kolade Koriko and Isaac Lare Animasaun. Modified kinematic viscosity model for 3D-Casson fluid flow within boundary layer formed on a surface at absolute zero. Journal of Molecular liquids 221 (2016) 1197-1206.
[3]. C. Sulochana, G.P. Ashwinkumar and N.Sandeep. Similarity solution of 3D Casson nanofluid flow over a stretching sheet with convective boundary conditions. Journal of the Nigerian Mathematical Society 35 (2016) 128-141.
[4]. N.Sandeep, Effect of Aligned Magnetic field on liquid thin film flow of magnetic-nanofluid embedded with graphene nanoparticles, Advanced Powder Technology, 28 (2017) 865–875.
[5]. M.Jayachandra Babu, N.Sandeep, UCM flow across a melting surface in the presence of double stratification and cross-diffusion effects, Journal of Molecular Liquids, 232 (2017) 27-35.
[6]. O.K.Koriko, A.J.Omowaye, N.Sandeep, I.L.Animasaun, Analysis of boundary layer formed on an upper horizontal surface of a paraboloid of revolution within nanofluid flow in the presence of thermophoresis and Brownian motion of 29 nm, International Journal of Mechanical Sciences, 124-125 (2017) 22-36.
[7]. G.Kumaran, N.Sandeep, Thermophoresis and Brownian moment effects on parabolic flow of MHD Casson and Williamson fluids with cross diffusion, Journal of Molecular Liquids, (Accepted), 2017.
[8]. J.V. Ramana Reddy, V. Sugunamma, N. Sandeep, Effect of frictional heating on radiative ferrofluid flow over a slendering stretching sheet with aligned magnetic field, Europen Physical Journal Plus, 132: 7, 2017.
[9]. G.Kumaran, N.Sandeep, M.E.Ali, Computational analysis of magneto-hydrodynamic Casson and Maxwell flows over a stretching sheet with cross diffusion, Results in Physics, 7 (2017)147-155.
[10]. M.E.Ali, N.Sandeep, Cattaneo-Christov model for radiative heat transfer of magnetohydrodynamic Casson-ferrofluid, Results in Physics 7 (2017) 21-30
[11] I.L.Animasaun, N.Sandeep, Buoyancy induced model for the flow of 36nm alumina-water nanofluid along upper horizontal surface of a paraboloid of revolution with variable thermal conductivity and viscosity, Powder Technology, 301,858-867, 2016.
[12] M.Jayachandra Babu, N.Sandeep, Three-dimensional MHD slip flow of a nanofluid over a slendering stretching sheet with thermophoresis and Brownian motion effects, Advanced Powder Technology, 27 (2016) 2039-2050.
[13]. N. Sandeep, A. Malvandi, Enhanced heat transfer in liquid thin film flow of non-Newtonian nanofluids embedded with grapheme nanoparticles, Advanced Powder Technology, 27(6) (2016) 2448-2456.
[14]. T. Hayat, S. Asad, A. Alsaedi, Flow of Casson fluid with nanoparticles, Applied Mathematics and Mechanics 37(4) (2016) 459-470.
[15]. T. Hayat, S.A. Shehzad, A. Alsaedi, M.S. Alhothuli, Mixed Convective Stagnation point flow of Casson fluid with convective boundary condition, Chin Phys Lett 29(2012) 256-307.
[16]. Nadeem .S, Haq Rizwan UI, Akbar NS, Khan ZH, MHD three-dimensional Casson fluid flow past a porous linearly stretching sheet, Alex. Eng. J. 52(2013) 577-682.
[17]. S. Pramanik, Casson fluid flow and heat transfer past an exponentially porous stretching sheet in the presence of thermal radiation, Ain Shams Eng J. 5(2014) 205-212.
[18]. G. Sarojamma, B. Vasundhara, K. Vendabai, MHD Casson Fluid Flow , Heat and Mass Transfer in a vertical channel with stretching walls, Int. J. Sci. Inno. Math. Res. 2(10), (2014) 800-810.
[19]. Emmanuel Maurice Arthur, Ibrahim Yakubu Seini, Letis Bortey, Analysis of Casson Fluid Flow over a vertical porous surface with Chemical Reaction in the presence of Magnetic Field, Journal of App. Math. and Phys. 3 (2015) 713-723.
[20].N.Sandeep, M.Gnaneswar Reddy, Heat transfer of nonlinear radiative magnetohydrodynamic Cu-water nanofluid flow over two different geometries, Journal of Molecular Liquids, 225, 87-94, 2017.
[21]. S. Harinath Reddy, M.C. Raju, E. Keshava Reddy, Radiation absorption and chemical reaction effects on MHD flow of Heat generating Casson fluid past an Oscillating vertical porous plate, Frontiers in Heat and Mass Transfer (FHMT), 7,21(2016).
[22]. A. Haritha, G. Sarojamma, Radiation effect on Heat and Mass Transfer in MHD flow of aCasson fluid over a stretching surface, Int. J. Sci. Inno. Math. Res. 2,6(2014) 546-553.
[23]. P.Sathies Kumar, K.Gangadhar, Three-dimensional MHD flow of a Casson fluid over a permeable Axisymmetric shrinking sheet with Heat Generation or absorption and Slip Velocity , IOSR Journal of Mathematics, 12 (3) (2016) 43-60.
[24]. Kankanala Sharada, Bandari Shankar, MHD mixed convection flow of a Casson fluid over an exponentially stretching surface with the effects of Soret, Dufour, thermal radiation and chemical reaction, World Journal of Mechanics, 2015, 5,165-177.

[25]. P. Nagarani, Peristaltic transport of a Casson fluid in an inclined channel, Korea-Australia Rheology Journal 22,2(2010) 105-111.
[26]. S. Ganesh, C.K. Kirubhashankar, A. Mohamed Ismail, Non-Linear Squeezing Flow of Casson Fluid between parallel plates, Int.J.Math.Analysis 9(2015) 5, 217-223.
[27]. G. Mahanta, S. Shaw, Mixed convection stagnation point flow of Casson fluid with Convective Boundary Conditions, Int.J.Inno.Res. in Sci., Eng and Tech. 4, 2(2015).
[28]. C.K. Kirubhashankar, S. Ganesh, A. Mohamed Ismail, Casson fluid flow and Heat Transfer over an unsteady porous stretching surface, Applied Mathematical Sciences, 9,(2015) 7, 345-351.
[29]. A. Mahdy, A. Chamkha, Heat transfer and fluid flow of a non-Newtonian nanofluid over an unsteady contracting cylinder employing Buongiorno's model, International Journals of Numerical methods for Heat and Fluid Flow 25, 4(2015), 703-723.
[30]. N. Vedavathi, G. Dharmaiah, K.S. Balamurugan, G. Charan Kumar, Chemical Reaction , Radiation and Dufour effectson Casson MHD Fluid Flow over a vertical plate with Heat source/sink, Global Journal of Pure and Applied Mathematics, 12, 1(2016), 191-200.
[31]. Md. Afikuzzaman, M. Ferdows and Md. Mahmud Alam, Unsteady MHD Casson Fluid Flow through a parallel plate with Hall Current, Procedia Engineering 105(2015) 287-293.
[32]. Naveed Ahmed, Umar Khan, Sheikh Irfanullah Khan, Saima Bano, Syed Tauseef Mohyud-Din, Effects on magnetic field in Squeezing flow of a Casson fluid between parallel plates, Journal of King Saud University-Science 29 (2017) 119-125.
[33]. N.Sandeep, S.Saleem, MHD flow and heat transfer of a dusty nano fluid over a stretching surface in porous medium, Jordan Journal of Civil Engineering, 11 (2017) 149-164.
[34]. M.Jayachandra Babu, N.Sandeep, Effect of variable heat source/sink on chemically reacting 3D slip flow caused by a slendering stretching sheet, Int. J. Eng. Research in Africa, 25 (2016) 58-69.
[35]. J.V.Ramana Reddy, V.Sugunamma, N.Sandeep, K. Anantha Kumar, Influence of non-uniform heat source/sink on MHD nanofluid flow past a slandering stretching sheet with slip effects, Global J. Pure and Applied Mathematics, 12 (2016) 247-254.
[36]. N.Sandeep, C.Sulochana, I.L.Animasaun, Stagnation-point flow of a Jeffrey nano fluid over a stretching surface with induced magnetic field and chemical reaction, Int.J.Eng. Resaech in Afrika, 20 (2016) 93-111.